Mechanism of Asymmetric Hydrogenation Catalyzed by a Rhodium Complex of (*S*,*S*)-1,2-Bis(*tert*-butylmethylphosphino)ethane. Dihydride Mechanism of Asymmetric Hydrogenation

Ilya D. Gridnev,* Natsuka Higashi, Katsuo Asakura, and Tsuneo Imamoto*

Contribution from the Department of Chemistry, Faculty of Science, Chiba University, Yayoi-cho, Inage-ku, Chiba 263-8522, Japan

Received March 6, 2000

Abstract: The mechanism of asymmetric hydrogenation catalyzed by a new effective catalyst, *viz.*, a rhodium complex of (*S*,*S*)-1,2-bis(*tert*-butylmethylphosphino)ethane (BisP*), has been studied by multinuclear NMR. Hydrogenation of the precatalyst [Rh(BisP*)(nbd)]BF_4 (**8**) at −20 °C in deuteriomethanol affords solvate complex [Rh(BisP*)$(CD_3OD)_2$]BF_4 (**9**), which is, in turn, hydrogenated at −90 °C producing equilibrium amounts (20% at −95 °C) of [RhH_2(BisP*)$(CD_3OD)_2$] (**10**)—the first observable dihydride of a Rh(I) complex with a diphosphine ligand. Dihydride **10** is in equilibrium with **9** and dihydrogen, which was studied in the temperature interval from −100 to −50 °C, yielding thermodynamic parameters $\Delta H = -6.3 \pm 0.2$ kcal M^{-1} and $\Delta S = -23.7 \pm 0.7$ cal M^{-1} K^{-1}. The hydrogenation of **9** is stereoselective: two isomers **10a** and **10b** are produced in a ratio 10:1. Use of HD for the hydrogenation of **9** yields the isomers with deuterium *cis* and *trans* to the phosphine in a ratio 1.3 (±0.1):1. The thermodynamic parameters of the equilibrium between **9**, **10d**, and HD are $\Delta H = -10.0 \pm 0.4$ kcal M^{-1} and $\Delta S = -20.3 \pm 1$ cal M^{-1} K^{-1}. Dihydride **10** reacts with the substrate **12** at −90 °C, yielding the monohydride intermediate **17a**. The same product is obtained when **13** is hydrogenated at −80 °C. At temperatures above −50 °C monohydride intermediate **17a** undergoes reductive elimination, affording the hydrogenation product **15** in equilibrium with the product−catalyst complex **16** in which the catalyst is η^6-coordinated to the phenyl ring of the product. The experimental data require that the dihydride mechanism is operating in the case of asymmetric hydrogenation catalyzed by **9**. This, in turn, suggests that the enantioselective step is the migratory insertion in a dihydride intermediate **18**.

Introduction

Mechanistic studies in the field of asymmetric hydrogenation of prochiral olefins have already a three-decade history.[1] In 1965 Wilkinson et al. reported that, upon hydrogenation of Wilkinson catalyst $RhCl(PPh_3)_3$, stable dihydride complex $RhH_2Cl(PPh_3)_3$ is produced.[2] It was concluded that hydrogenation of the catalyst precedes the coordination of the substrate.[3] Later studies have provided experimental evidence for certain stages of the catalytic cycle[4−8] and revealed the complicated nature of the system consisting of $RhCl(PPh_3)_3$, dihydrogen, and olefin.[5,7−9]

Discovery of the high synthetic potential of rhodium(I) complexes containing chiral diphosphines in asymmetric hydrogenation[10−21] promoted mechanistic studies. In contrast to the Wilkinson catalyst, no stable hydride complexes were detected upon hydrogenation of [Rh(dppe)(nbd)]BF_4 (**1**).[22] Instead, dimer **2** has been structurally characterized, which dissociates in solution producing solvate complex **3** (Scheme 1).[22] Note, however, that *ortho*−*para* hydrogen exchange experiments indicated the existence of a nondetectable concentration of a dihydride in equilibrium with **3**.[23]

Further work showed that formation of the complexes of the type **3** upon hydrogenation of a catalytic precursor is a general

(1) Brown, J. M. *Hydrogenation of Functionalized Carbon−Carbon Double Bonds*; Jacobsen, E. N., Pfaltz, A., Yamamoto, H., Eds.; Springer: Berlin, 1999; Vol. 1, pp 119−182.
(2) Young, J. F.; Osborn, J. A.; Jardine, F. H.; Wilkinson, G. *Chem. Commun.* **1965**, 131−132.
(3) Osborn, J. A.; Jardine, F. H.; Young, J. F.; Wilkinson, G. *J. Chem. Soc. A* **1966**, 1711−1732.
(4) Halpern, J.; Wong, C. S. *J. Chem. Soc., Chem. Commun.* **1973**, 629−630.
(5) Tolman, C. A.; Meakin, P. Z.; Lindner, D. L.; Jesson, J. P. *J. Am. Chem. Soc.* **1974**, *96*, 2762−2774.
(6) Halpern, J.; Okamoto, T.; Zakhariev, A. *J. Mol. Catal.* **1976**, *2*, 65−68.
(7) Brown, J. M.; Evans, P. L.; Lucy, A. R. *J. Chem. Soc., Perkin Trans. 2* **1987**, 1589−1596.
(8) Duckett, S. B.; Newell, C. L.; Eisenberg, R. *J. Am. Chem. Soc.* **1994**, *116*, 10548−10556.
(9) Brown, J. M.; Chaloner, P. A.; Nicholson, P. N. *J. Chem. Soc., Chem. Commun.* **1978**, 646−647.
(10) Dang, T. P.; Kagan, H. B. *Chem. Commun.* **1971**, 481.
(11) Knowles, W. S.; Sabacky, M. J.; Vineyard, B. D. *J. Chem. Soc., Chem. Commun.* **1972**, 10−11.
(12) Kagan, H. B.; Dang, T. P. *J. Am. Chem. Soc.* **1972**, *94*, 6429−6433.
(13) Knowles, W. S.; Sabackky, M. J.; Vineyard, B. D.; Weinkauff, D. J. *J. Am. Chem. Soc.* **1975**, *97*, 2567−2568.
(14) Kagan, H. B.; Langlois, N.; Dang, T. P. *J. Organomet. Chem.* **1975**, *90*, 353−365.
(15) Tanaka, M.; Ogata, I. *J. Chem. Soc., Chem. Commun.* **1975**, 735.
(16) Gelbard, G.; Kagan, H. B.; Stern, R. *Tetrahedron* **1976**, *32*, 233−237.
(17) Achiwa, K. *J. Am. Chem. Soc.* **1976**, *98*, 8265−8266.
(18) Kawabata, Y.; Tanaka, M.; Ogata, I. *Chem. Lett.* **1976**, 1213−1214.
(19) Hayashi, T.; Mise, T.; Mitachi, S.; Yamamoto, K.; Kumada, M. *Tetrahedron Lett.* **1976**, 1133−1134.
(20) Vineyard, B. D.; Knowles, W. S.; Sabacky, G. L.; Bachman, G. L.; Weinkauff, D. J. *J. Am. Chem. Soc.* **1977**, *99*, 5946−5952.
(21) Fryzuk, M. D.; Bosnich, B. *J. Am. Chem. Soc.* **1977**, *99*, 6262−6267.
(22) Halpern, J.; Riley, D. P.; Chan, A. S. C.; Pluth, J. J. *J. Am. Chem. Soc.* **1977**, *99*, 8055−8057.
(23) Brown, J. M.; Canning, L. R.; Downs, A. R.; Forster, A. M. *J. Organomet. Chem.* **1983**, *255*, 103−111.

10.1021/ja000813n CCC: $19.00
Published on Web 07/18/2000

Scheme 1

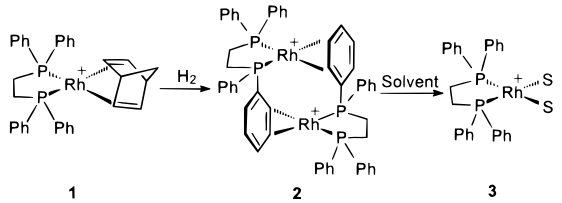

phenomenon for the rhodium(I) complexes containing various diphosphine ligands.[24−31] Usually, no hydride complexes were detected in the solutions of solvates **3** under hydrogen; hydride intermediates or oligomeric solvates have been noticed only when the diphosphine ligand was capable of *trans*-coordination.[29,32] Note also the formation of an unusual binuclear trihydride complex with bridging perchlorate anion.[33,34]

It has been concluded, therefore, that the hydrogenation stage occurs after substrate binding in the case of *cis*-chelating diphosphine rhodium complexes, and the catalytic cycle for unsaturated mechanism (Scheme 2) has been proposed.[22,26,35−37] This point of view is now generally accepted, although the alternative mechanisms are considered, at least theoretically.[1,38−40] The possibility of the dihydride mechanism in which the catalyst first reacts with hydrogen has been discussed in the case of *trans*-binding ligands[41,42] or at high pressures of hydrogen.[28]

Numerous catalyst−substrate complexes of the type **4** have been characterized by spectroscopic methods[24,26−28,30,31,43−53] and

Scheme 2

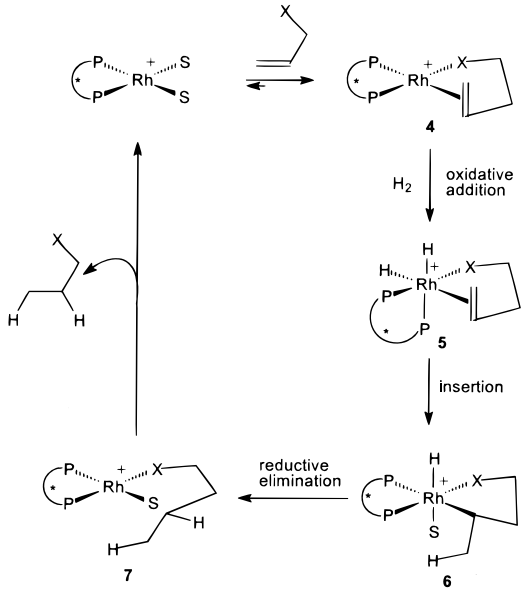

by X-ray analyses.[22,26,54] In the case of a chiral diphosphine ligand, several diastereomers of catalyst−substrate complex **4** are possible (two in the case of C_2-symmetrical ligand and four in the case of unsymmetrical diphosphines), but often only one diastereomer predominates in solution. Initially, it had been assumed that the stereochemistry of hydrogenation may be mainly regulated by the relative thermodynamic stability of one diastereomer.[24,27,28,55] However, X-ray structure[26] and comparative study of the solution and solid-state CD spectra[56] of the complex **4** containing CHIRAPHOS as a ligand and ethyl (*Z*)-α-acetamidocinnamate as a substrate showed that the configuration of the major diastereomer does not correspond to the configuration of the product, if *endo*-addition of H_2 is assumed. Moreover, it was found that when the catalyst−substrate complex **4** of $[Rh(DIPAMP)]^+$ with methyl (*Z*)-α-acetamidocinnamate is hydrogenated at low temperatures, the reactivity of the minor (less stable) diastereomer toward hydrogen is notably higher compared to the major (more stable) diastereomer.[43] These findings led to the conclusion[37] that at least in these two cases (CHIRAPHOS and DIPAMP) the stereochemistry of hydrogenation is regulated by the relative reactivity of two diastereomers of **4** rather than by their relative abundance in the equilibrium.

In this respect, the rate and the mechanism of interconversion of the diastereomers are very important, since if the rate of oxidative addition of hydrogen is greater than the rate of diastereomers interconversion, the optical yields should decrease. Thus, the decrease of ee's under high pressure of H_2[28,57] or at low temperatures[37] has been explained in this fashion.

Interconversion of diastereomers **4a** and **4b** can occur either inter-[48,50] or intramolecularly[47,50] (Scheme 3). In the most recent

(24) Brown, J. M.; Chalonter, P. A. *Tetrahedron Lett.* **1978,** 1877−1880.
(25) Slack, D. A.; Greveling, I.; Baird, M. C. *Inorg. Chem.* **1979**, *18*, 8, 3125−3132.
(26) Chan, A. S. S.; Pluth, J. J.; Halpern, J. *J. Am. Chem. Soc.* **1980**, *102*, 5952−5954.
(27) Brown, J. M.; Chaloner, P. A. *J. Am. Chem. Soc.* **1980**, *102*, 3040−3048.
(28) Ojima, I.; Kogure, T.; Yoda, N. *J. Org. Chem.* **1980**, *45*, 4728−4739.
(29) Brown, J. M.; Chaloner, P. A.; Kent, A. G.; Murrer, B. A.; Nicholson, P. N.; Parker, D.; Sidebottom, P. J. *J. Organomet. Chem.* **1981**, *216*, 263−276.
(30) Miyashita, A.; Takaya, H.; Souchi, T.; Noyori, R. *Tetrahedron* **1984**, *40*, 1245−1253.
(31) Allen, D. G.; Wild, S. B.; Wood, D. L. *Organometallics* **1986**, *5*, 1009−1015.
(32) Descotes, G.; Lafont, D.; Sinou, D.; Brown, J. M.; Chaloner, P. A.; Parker, D. *Nouv. J. Chim.* **1981**, *5*, 167−173.
(33) Tani, K.; Suwa, K.; Yamagata, T.; Otsuka, S. *Chem. Lett.* **1982**, 265−268.
(34) Tani, K.; Yamagata, T.; Tatsuno, Y.; Saito, T.; Yamagata, Y.; Yasuoka, N. *J. Chem. Soc., Chem. Commun.* **1986**, 494−495.
(35) Chan, A. S. C.; Halpern, J. *J. Am. Chem. Soc.* **1980**, *102*, 838−840.
(36) Chan, A. S. C.; Pluth, J. J.; Halpern, J. *Inorg. Chim. Acta* **1979**, *37*, L477−L479.
(37) Halpern, J. *Science* **1982**, *217*, 401−407.
(38) Brown, J. M. *Chem. Soc. Rev.* **1993**, *22*, 25−41.
(39) Noyori, R. *Asymmetric Catalysis in Organic Synthesis*; John Wiley & Sons: New York, 1994.
(40) Landis, C. R.; Hilfenhaus, P.; Feldgus, S. *J. Am. Chem. Soc.* **1999**, *121*, 8741−8754.
(41) Sinou, D. *Tetrahedron Lett.* **1981**, *22*, 2987−2990.
(42) Kuwano, R.; Ito, Y. *J. Org. Chem.* **1999**, *64*, 1232−1237.
(43) Brown, J. M.; Chaloner, P. A. *J. Chem. Soc., Chem. Commun.* **1980**, 344−346.
(44) Brown, J. M.; Parker, D. *J. Chem. Soc., Chem. Commun.* **1980**, 342−344.
(45) Brown, J. M.; Parker, D. *J. Org. Chem.* **1982**, *47*, 2722−2730.
(46) Brown, J. M.; Chalonter, P. A.; Morris, G. A. *J. Chem. Soc., Chem. Commun.* **1983**, 664−666.
(47) Brown, J. M.; Chaloner, P. A. *J. Chem. Soc., Perkin Trans. II* **1987**, 1583−1588.
(48) Landis, C. R.; Halpern, J. *J. Am. Chem. Soc.* **1987**, *109*, 1746−1754.
(49) Bender, B. R.; Koller, M.; Nanz, D.; Philipsborn, W. v. *J. Am. Chem. Soc.* **1993**, *115*, 5889−5890.
(50) Bircher, H.; Bender, B. R.; Philipsborn, W. v. *Magn. Reson. Chem.* **1993**, *31*, 293−298.
(51) Giovannetti, J. S.; Kelly, C. M.; Landis, C. R. *J. Am. Chem. Soc.* **1993**, *115*, 4040−4057.
(52) Kadyrov, R.; Freier, T.; Heller, D.; Michalik, M.; Selke, R. *J. Chem. Soc., Chem. Commun.* **1995**, 1745−1746.
(53) RajanBabu, T. V.; Radetich, B.; Kamfia, K. Y.; Ayers, T. A.; Casalnuvo, A. L.; Calabrese, J. C. *J. Org. Chem.* **1999**, *64*, 3429−3447.
(54) McCulloh, B.; Halpern, J.; Thompson, M. R.; Landis, C. R. *Organometallics* **1990**, *9*, 1392−1395.
(55) Brown, J. M.; Chaloner, P. A. *J. Chem. Soc., Chem. Commun.* **1978**, 321−322.
(56) Chua, P. S.; Roberts, N. K.; Bosnich, B.; Okrasinski, S. J.; Halpern, J. *J. Chem. Soc., Chem. Commun.* **1981**, 1278−1280.
(57) Ojima, I.; Kogure, T. *Chem. Lett.* **1979**, 495−499.

Scheme 3

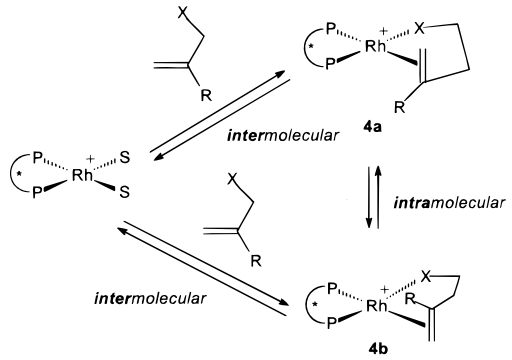

study, a mixed mechanism has been actually proposed.[50] In seven-membered ring chelates of rhodium-bis(phosphinites), both reaction pathways are fast in the NMR time scale at room temperature; low-temperature experiments have shown, however, that the intramolecular isomerization proceeds faster.[52]

Although the hydridoalkyl intermediates **6** (Scheme 2) have previously been characterized by NMR in 1980,[35,43] the reality of the dihydride intermediates **5** in the asymmetric hydrogenation has been experimentally demonstrated only recently.[58] However, their structure remains unclear, since from the ^{1}H NMR data neither of the hydrides seems to be *trans* to phosphorus. This result has been interpreted by the distorted octahedral geometry of the dihydride intermediates.[58]

The difference in the reactivity of **4a** and **4b** toward hydrogen cannot be adequately rationalized.[48,53] Discussions of this problem are often speculative.[49,59] Early computational studies of the pathways and transition states of H_2 oxidative addition to diastereomers of **4**[60−62] inevitably relied on the solid-state structures of the catalytic precursors and long remained below the molecular mechanics level due to the absence of reliable force field constants for metal complexes. Recently, the DFT calculations of the model nonchiral complexes were reported.[40] Two important modifications of the unsaturated mechanism follow from these results: (1) the importance of molecular hydrogen complexes as the intermediates in H_2 oxidative addition to the catalyst-substrate complexes; (2) the rate-turnover step is the migratory insertion rather than the oxidative addition. However, the authors admit that the real systems containing bulky substituents may differ significantly from the model complexes studied so far.[40]

Since the exact mechanistic model for the origin of stereoselection is still unavailable, empirical rules for the prediction of the stereochemical outcome of a hydrogenation catalyzed by a certain Rh(I)−diphosphine complex have been proposed. Historically Fryzuk and Bosnich noticed at first that the stable conformations (in which the methyl groups are quasi-equatorial) of the Rh chelate rings with *S,S*-CHIRAPHOS[21] and *R*-PROPHOS[63] are chiral and different (δ- and λ-conformations, respectively). Accordingly, these complexes give in hydrogenation *R*- and *S*-amino acids. Similar observations were made by Kagan for PHELLANPHOS and NOPAPHOS ligands.[64] Later, a considerable amount of X-ray data was found to be in accord with this empirical rule.[65] Two related rules[66,67] apparenly refer to the same stereochemical regularities.

An alternative approach for the prediction of the stereochemical result of the hydrogenation has been developed by Knowles et al.[68,69] This approach operates with "quardant diagrams" for representation of the chiral environment of the rhodium atom. Since in the case of the mostly studied tetraphenyl-substituted diphosphine ligands with a chiral backbone, all four substituents are equivalent, the "quadrant rule" regards the *edge*- and *face*-oriented phenyls at the phosphorus atoms in the solid-state structures of the catalytic precursors as the main stereoregulating factors.

These rules are not valid for many of the new catalysts with electron-rich diphosphine ligands. Thus, the catalytic precursor [Rh((*S,S*)-*t*-Bu-BisP*)(nbd)]BF_4 (**8**) is λ-shaped but gives *R*-amino acids with extremely high ee's.[70] The λ,δ rule cannot be applied to the flat [Rh((*R,R*)-Me-DuPHOS)(cod)]SbF_6[71] or [Rh((*R,R*)-*t*-Bu-MiniPHOS)$_2$]PF_6,[72] but application of the quadrant rule leads to wrong predictions. The same is valid for the Rh complexes of the newly designed BPE,[71] BIPNOR,[73] CnrPHOS,[74,75] and BisP*[70]diphosphine ligands.

Neither can the twist of the coordinated diene[76] in **8** be correlated with the sense of enantioselection, since the diene molecule is symmetrically coordinated in **8**[70] despite the apparent difference in size of the methyl and *tert*-butyl substituents on phosphorus.

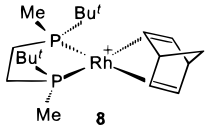

8

Almost all mechanistic studies of catalytic asymmetric hydrogenation have been carried out for the catalysts with bis(diarylalkylphosphine) ligands. We are only aware of the work of Armstrong, Brown, and Burk on the catalyst−substrate complexes with (*S,S*)-Me-DuPHOS ligand largely made for Ir complexes.[77] Besides, very recently, Burk et al. have published some experimental results demonstrating the importance of the carboxylate function for the effective asymmetric reduction of a precursor of candoxantril with (*R,R*)-Me-DuPHOS−Rh cata-

(58) Harthun, A.; Kadyrov, R.; Selke, R.; Bargon, J. *Angew. Chem., Int. Ed. Engl.* **1997**, *36*, 1103−1105.
(59) Nagel, U.; Rieger, B. *Organometallics* **1989**, *8*, 1534−1538.
(60) Arriau, J.; Fernandez, J.; Melendez, E. *J. Chem. Res., Synop.* **1984**, 106−107.
(61) Brown, J. M.; Evans, P. L. *Tetrahedron* **1988**, *44*, 4905−4916.
(62) Bogdan, P. L.; Irwin, J. J.; Bosnich, B. *Organometallics* **1989**, *8*, 1450−1453.
(63) Fryzuk, M. D.; Bosnich, B. *J. Am. Chem. Soc.* **1978**, *100*, 5491−5494.
(64) Samuel, O.; Couffignal, R.; Lauer, M.; Zhang, S. Y.; Kagan, H. B. *Nouv. J. Chem.* **1981**, *5*, 15−20.
(65) Kagan, H. B. *Asymmetric synthesis using organometallic catalysts*; Wilkinson, G., Stone, F. G. A., Abel, E. W., Eds.; Pergamon: Oxford, 1982; Vol. 8, pp 463−498.
(66) Pavlov, V. A.; Klabunovskii, E. I.; Struchkov, Y. T.; Voloboev, A. A.; Yanovsky, A. I. *J. Mol. Catal.* **1988**, *44*, 217−243.
(67) Sakuraba, S.; Morimoto, T.; Achiwa, K. *Tetrahedron: Asymmetry* **1991**, *2*, 597−600.
(68) Koenig, K. E.; Sabacky, M. J.; Bachman, G. L.; Christopfel, W. C.; Barnstorff, H. D.; Friedman, R. B.; Knowles, W. S.; Stults, B. R.; Vineyard, B. D.; Weinkauff, D. J. *Ann. N.Y. Acad. Sci.* **1980**, *333*, 16−22.
(69) Knowles, W. S. *Acc. Chem. Res.* **1983**, *16*, 106−112.
(70) Imamoto, T.; Watanabe, J.; Wada, Y.; Masuda, H.; Yamada, H.; Tsuruta, H.; Matsukawa, S.; Yamaguchi, K. *J. Am. Chem. Soc.* **1998**, *120*, 1635−1636.
(71) Burk, M. J.; Feaster, J. E.; Nugent, W. A.; Harlow, R. L. *J. Am. Chem. Soc.* **1993**, *115*, 10125−10138.
(72) Yamanoi, Y.; Imamoto, T. *J. Org. Chem.* **1999**, *64*, 2988−2989.
(73) Robin, F.; Mercier, F.; Ricard, L.; Mathey, F.; Spagnol, M. *Chem. Eur. J.* **1997**, *3*, 1365−1369.
(74) Marinetti, A.; Jus, S.; Genet, J.-P. *Tetrahedron Lett.* **1999**, *40*, 8365−8368.
(75) Martinetti, A.; Kruger, Y.; Buzin, F. X. *Tetrahedron Lett.* **1997**, *38*, 2947−2950.
(76) Kyba, E. P.; Davis, R. E.; Juri, P. N.; Shirley, K. R. *Inorg. Chem.* **1981**, *20*, 3616−3623.
(77) Armstrong, S. K.; Brown, J. M.; Burk, M. J. *Tetrahedron Lett.* **1993**, *34*, 879−882.

Scheme 4

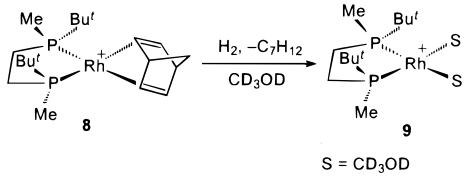

Scheme 5

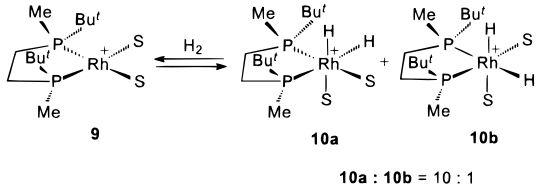

lyst.[78] However, neither the reasons for the unusually high activity of the bis(trialkylphosphine)-based catalysts nor the above outlined apparent difficulties in application of the stereoselection rules to these catalysts are understood or even have been challenged until now. We therefore undertook a detailed study of the mechanism of catalytic asymmetric hydrogenation catalyzed by (*S,S*)-*t*-Bu-BisP*−Rh catalyst.

Results and Discussion

1. Hydrogenation of the Precatalyst. (a) Formation of Solvate Complex 9. Like all other known catalytic precursors, [Rh(BisP*)(nbd)]BF_4 **8** is easily hydrogenated in deuteriomethanol at −20 °C to produce a solvate complex [Rh (BisP*)$(CD_3OD)_2$]BF_4 (**9**) (Scheme 4). Complex **9** was characterized by its ^{1}H, ^{13}C, and ^{31}P NMR spectra. In the ^{31}P NMR spectrum a dublet was found ($\delta = 89.8$, $^1J_{P-Rh} = 204$ Hz). In the ^{13}C NMR spectrum three multiplets with characteristic splitting patterns for the A parts of the AXYY′ system were observed together with the intensive singlet of 6 methyls from 2 *t*-Bu groups ($\delta = 27.3$). The multiplets are easily attributable to the signals of the P-methyl groups ($\delta = 10.7$), CH_2 group ($\delta = 25.4$), and quartenary carbons ($\delta = 32.4$), respectively. The positions of three multiplets corresponding to *t*-Bu, Me, and CH_2 groups in the ^{1}H NMR spectrum were verified by 2D heteronuclear ^{13}C−^{1}H and ^{31}P−^{1}H correlations.

(b) Oxidative Addition of H_2 to Solvate Complex 9. We found that solvate complex **9** reacted with dihydrogen reversibly and stereoselectively, producing two isomers of the dihydride **10** in the ratio 10:1 (Scheme 5). The relatively high concentrations of dihydride **10** (approximately 20 mol %) were obtained when **9** generated by hydrogenation of **8** at −50 °C was further hydrogenated at −90 °C for 30 min.

In the hydride region of the proton spectrum (Figures 1 and 2) two 16-line multiplets were observed at −7.7 and −23.0 ppm. These protons are coupled through the 5 Hz coupling as follows from the homodecoupling experiments. The same absolute value of the geminal proton−proton coupling in a Rh dihydride has been recently reported.[79] The minor isomer **10b** gives two multiplets similar to those of **10a** at −7.0 and −23.1 ppm. The ^{31}P NMR spectrum of the hydrogenation product (Figure 1) contains two doublets at $\delta = 43.8$ (^1J(P, Rh) = 86 Hz) and $\delta = 95.0$ (^1J(P, Rh) = 145 Hz). Each of these two signals correlates with both hydride protons in the 2D P, H correlation experiments. The coupling $^2J(P^A,P^B)$ is less than 5 Hz, which resembles the very small ^2J(P, P) couplings in a rhodium cationic complex $[RhH_2(PP_3)]^+$ ($PP_3 = P(CH_2CH_2PPh_2)_3$).[79−81]

Further details of the hydrides spin systems were clarified by the selective ^{31}P decoupling experiments (Figure 2, Table S1). Thus, the large 186 Hz coupling of the signal at −7.7 ppm disappeared when the high-field doublet in the ^{31}P spectrum was irradiated (Figure 2b). Irradiation of the doublet at $\delta = 95.0$ in the ^{31}P eliminated one of the two equal 19 Hz couplings in the same multiplet (Figure 2c). The remaining 19 Hz coupling is, therefore, with rhodium. Similarly, the details of the coupling patterns were found for the hydride signal at $\delta = -23.0$ and for the minor isomer of **10** (Table S1).

From the known starting concentration of **8** and the integral intensities of the signals of **9** and **10** (both isomers) in the ^{31}P NMR spectra, the absolute concentrations of **9** and **10** can be calculated. The concentration of dihydrogen in the solution could, in turn, be obtained from the relative intensities of the hydride signals of **9** and the signal of dihydrogen at $\delta = 4.5$. This allows calculation of the equilibrium constant $K = [\mathbf{10}]/[\mathbf{9}][H_2]$. The temperature dependence of ln *K* versus reverse temperature was linear in the temperature interval from −95 to −50 °C. The parameters of equilibrium obtained from these data are $\Delta H = -6.3 \pm 0.2$ kcal M^{-1} and $\Delta S = -23.7 \pm 0.7$ cal M^{-1} K^{-1}. We were able to observe only equilibrium concentrations of **10** even at −100 °C. Therefore, the rate of equilibration of **9** and **10** is higher than that reported recently for [Ir((*R,R*)-Me-DuPHOS)(cod)]BF_4.[84]

The relative stability of the dihydride **10** is most probably stipulated for the electron-rich character of the diphosphine ligand stabilizing the octahedral dihydride complex. This assumption is in accord with theoretical anticipations.[40,82]

In the ^{1}H 2D EXSY spectra taken in the temperature interval from −90 to −60 °C, intensive exchange cross-peaks between two hydride signals were observed. On the other hand, no exhange cross-peaks of hydride protons with dihydrogen were observed. Neither exchange cross-peaks were found in the ^{31}P 2D EXSY spectra taken in the same temperature interval. Therefore, the hydrides in **10** can interchange their positions without complete dissociation of the hydrogen. A similar conclusion has been recently made for a structurally related $[RhH_2(PP_3)]^+$ complex.[79] The mechanism suggested by Heinekey and van Roon on the basis of evaluated kinetic isototope effect implies the formation of an intermediate of the type **11** with substantial H−H interactions (Scheme 6). Quantification of the EXSY data obtained at two different mixing times at 193 K gave the rate constant $k = 1.4$ s^{-1} at this temperature. The exchange with complete elimination of dihydrogen is at least 10 times slower.

The intermediacy of dihydrogen complex **11** in the intramolecular dynamic rearrangement of **10** is also in accord with the most recent computational study of the oxidative H_2 addition to Rh(I) complexes.[40] Landis et al. have shown that the molecular hydrogen coomplexes are real minima on the potential energy surface for the hydrogenation of model Rh(I) phosphine

(78) Burk, M. G.; Bienewald, F.; Challenger, S.; Derrick, A.; Ramsden, J. A. *J. Org. Chem.* **1999**, *64*, 3290−3298.
(79) Heinekey, D. M.; Roon, M. v. *J. Am. Chem. Soc.* **1996**, *118*, 12134−12140.
(80) Bianchini, C.; Mealli, C.; Peruzzini, M.; Zanobini, F. *J. Am. Chem. Soc.* **1987**, *109*, 5548−5549.
(81) Biandini, C.; Elsevier, C. J.; Ernsting, J. M.; Peruzzini, M.; Zanobini, F. *Inorg. Chem.* **1995**, *34*, 84−92.
(82) Sargent, A. L.; Hall, M. B.; Guest, M. F. *J. Am. Chem. Soc.* **1992**, *114*, 517−522.
(83) Burk, M. J.; McGrath, M. P.; Wheeler, R.; Crabtree, R. H. *J. Am. Chem. Soc.* **1988**, *110*, 5034−5039.
(84) Kimmich, B. F. M.; Somsook, E.; Landis, C. R. *J. Am. Chem. Soc.* **1998**, *120*, 10115−10125.

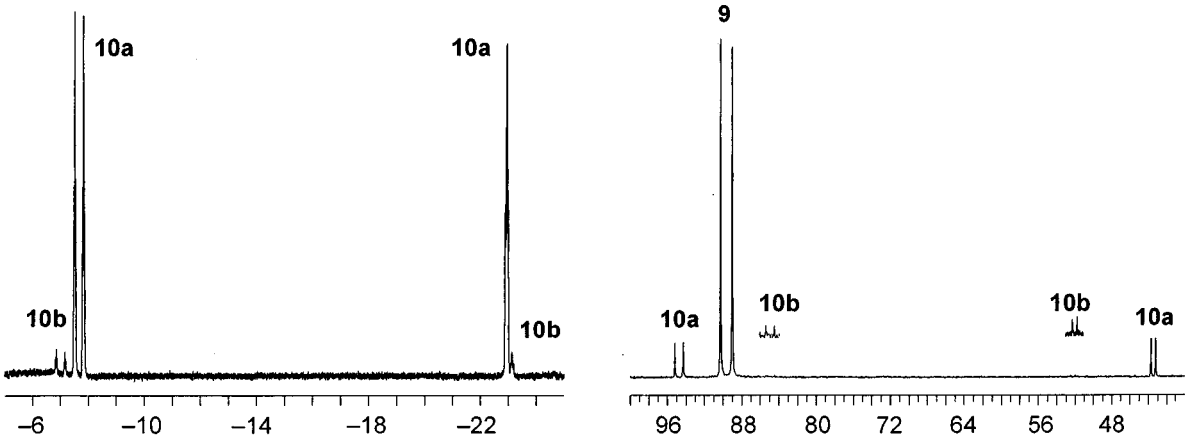

Figure 1. Left: hydride region of the ^{1}H NMR spectrum (600 MHz, CD_3OD, −90 °C) of the equilibrium mixture of **9** and **10**. Right: ^{31}P NMR spectrum (162 MHz, CD_3OD, −90 °C) of the equilibrium mixture of **9** and **10**.

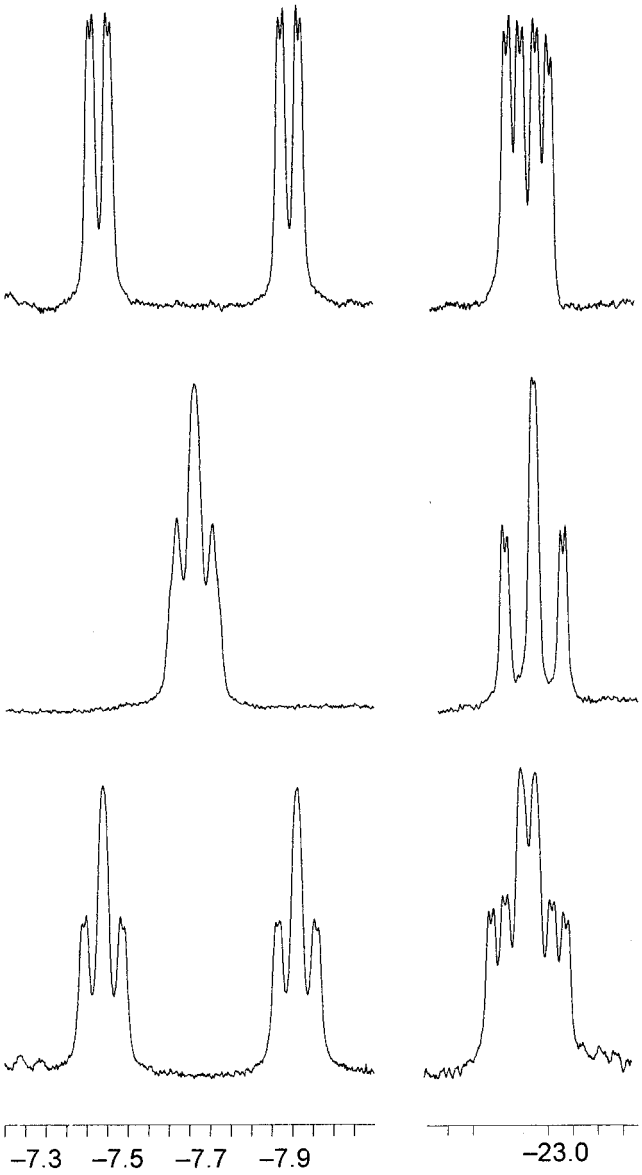

Figure 2. Line shape of the hydride signals of **10a** in the ^{1}H NMR spectra (400 MHz, CD_3OD, −70 °C): (a) normal ^{1}H NMR; (b) selective decoupling from ^{31}P with $\delta = 43.5$; (c) selective decoupling from ^{31}P with $\delta = 95.0$.

complexes and are comparable in energy with further formed dihydrides.[40]

Scheme 6

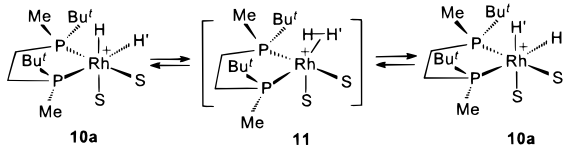

Scheme 7

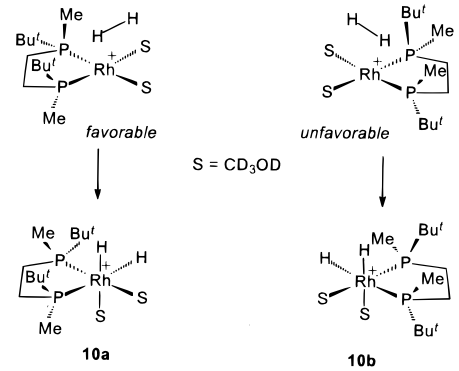

The selectivity in hydrogenations of transition metal complexes governed by the electronic properties of different ligands has been extensively studied.[82,83] However, in the hydrogenation of **9** the stereoselectivity is induced by the steric properties of the ligands. Similar high diastereoselectivity was recently observed for the hydrogenation of a series of Ir diphosphine complexes.[84]

We could not determine experimentally the structure of the major diastereomer, since the alkyl groups of **10** resonate very closely in the ^{1}H NMR spectrum. The molecule of the rhodium complex is C_2-symmetrical, and there are only two possibilities for the hydrogen molecule to approach it for the oxidative addition. One of these posibilities is evidently favored due to the less steric hindrance from the bulky *t*-Bu groups (Scheme 7). We think, therefore, that the formation of **10a** may be preferred kinetically. However, the relative thermodynamic stability of one of the diastereomers observed in our experiments is difficult to rationalize due to the very similar structures of **10a** and **10b**.

(c) Oxidative Addition of HD to the Solvate Complex 9. The hydrogenation of **9** using HD gave the mixture of four isomers **10^d** (Scheme 8). The ratio **10a^d**:**10b^d** was the same as for the corresponding dihydrides (10:1). Of interest is the significantly unequal distribution of deuterium between *cis* and

Scheme 8

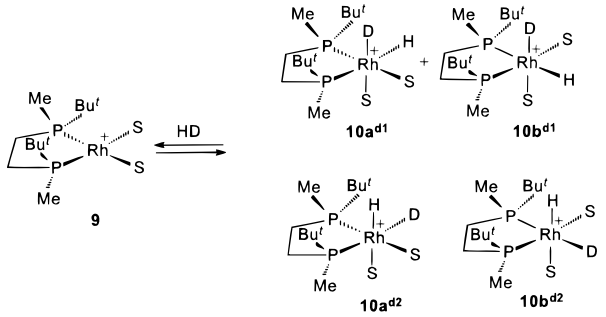

Scheme 9

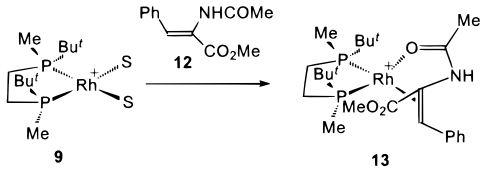

trans positions (relative to the phosphorus atom): deuterium prefers to occupy *cis* position with a factor 1.3 ± 0.1. The ratio (**10a^{d1}** + **10b^{d1}**):(**10a^{d2}** + **10b^{d2}**) remained constant within experimental error in the temperature interval from −100 to −50 °C and was reproduced exactly in four independent hydrogenation experiments. To our knowledge, this is a first observation of such effect for the oxidative addition of HD to transition metal complexes.[84]

The parameters of equilibrium between **9**, HD, and **10^{d}** (all isomers) have been found similarly to the equilibrium with H_2 (see above). The thermodynamic parameters of this equilibrium are $\Delta H = -10.0 \pm 0.4$ kcal M^{-1} and $\Delta S = -20.3 \pm 1$ cal M^{-1} K^{-1}. The significant equilibrium isotope effect observed for the addition of HD is in accord with known regularities.[85]

Thus, we have detected the reversible and stereoselective formation of the dihydride complex **10** upon hydrogenation of the solvate complex **9** in deuteriomethanol. This observation gives reasons to consider a dihydride mechanism for the asymmetric hydrogenations catalyzed by **9**. To probe further this possibility, we have studied the asymmetric hydrogenation of methyl (*Z*)-α-acetamidocinnamate (**12**).

2. Binding of the Catalyst with a Substrate and a Hydrogenation Product. (a) NMR Study of the Solution Structure of a Catalyst−Substrate Complex. Addition of a 2-fold excess of methyl (*Z*)-α-acetamidocinnamate (**12**) to a solution of solvate complex **9** in deuteriomethanol under argon resulted in immediate formation of catalyst−substrate complex **13** (Scheme 9).

The ^{31}P NMR spectrum of the complex **13** at room temperature shows two signals at 76.0 and 79.3 ppm (Figure 3h, Table S2). Each is split by a large heteronuclear Rh−P coupling (158 and 156 Hz, respectively) and a smaller homonuclear P−P coupling (32 Hz). The results of the heteronucleus ^{31}P−^{1}H correlation experiments together with the NOESY data indicate that the high-field signal is *trans* to the double bond. This is in accord with the most recent assignments.[50]

In the ^{1}H NMR spectrum of **13** the olefinic proton resonates as double doublet at 6.08 ppm and has characteristic couplings $^{2}J_{HRh} = 3.0$ Hz and $^{3}J_{HP} = 4.9$ Hz (confirmed by the ^{31}P−^{1}H correlation and selective decoupling experiments). In the aliphatic part of the spectrum all four alkyl groups resonate separately due to lack of symmetry in the molecule of **13**. The four protons of two CH_2 groups give complex multiplets; their positions in the spectrum were found from 2D ^{1}H−^{13}C correlation experiments. The methyl groups of the diphosphine give doublets at 1.40 and 1.52 ppm, whereas the signals of two *t*-Bu groups are separated for 0.48 ppm ($\delta = 0.70$ and 1.18). The considerable high-field shift of one of the *t*-Bu groups (it is the *t*-Bu group attached to high-field phosphorus with $\delta = 76.0$ ppm according to the ^{31}P−^{1}H correlation) is caused by the well-known shielding effect of a spatially close phenyl ring. This conclusion has been confirmed by a comparison of the ^{1}H NMR spectrum of **13** with the ^{1}H NMR spectra of the complexes of **9** with (*Z*)-α-acetamidocinnamic acid ($\Delta\delta$(*t*-Bu) = 0.46), acetamidoacrylic acid ($\Delta\delta$(*t*-Bu) = −0.08), and dimethyl itaconate ($\Delta\delta$(*t*-Bu) = −0.08); these results will be reported in detail elsewhere.

Scheme 10

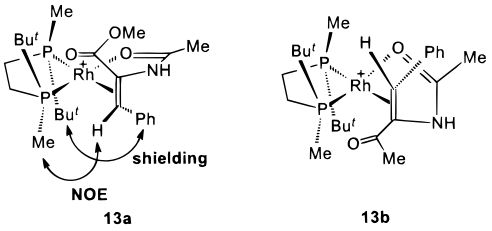

In the phase-sensitive NOESY spectrum of **13**, the intensive NOE cross-peak is observed between the olefinic proton of the substrate and the methyl group attached to the low-field phosphorus atom ($\delta = 79.3$). The intensity of this cross-peak is the same as for the evident cross-peak of the olefinic proton with *ortho*-protons of the adjacent phenyl ring. This NOE and the shielding of one *t*-Bu group taken together allow elucidation of the solution structure of the complex **13** (Scheme 10). Only in the case of diastereomer **13a** it is possible to obtain close proximity between one of the *t*-Bu groups and the phenyl ring under the condition that the methyl group *attached to another phosphorus atom* is close enough to the olefinic proton to produce NOE.

In the ^{13}C NMR spectrum of **13** (Table S3), both signals of the Rh-coordinated double bond have the expected couplings with *trans*-phosphorus, whereas the quarternary carbon atom is additionally coupled to rhodium (6 Hz). Both amide and carboxyl carbonyls are coupled to phosphorus as was previously observed for the DIPAMP complex.[27] Additionally a long-range coupling (3 Hz) with *trans*-phosphorus is observed for the quarternary aromatic carbon. In the aliphatic region of the ^{13}C NMR spectrum, two signals of the *t*-Bu methyls, two doublets of P-bonded methyls, and two doublets of quarternary carbons have the expected chemical shifts and couplings values. The CH_2 groups give multiplets at $\delta = 21.1$ and 32.6 (Table S3).

It should be noted that the solution structure of **13**, similarly to the catalyst−substrate complexes studied so far, does not correspond to the configuration of the hydrogenation product. Thus, olefin in **13a** is coordinated with its *re*-face, but the hydrogenation of **12** catalyzed by **9** gives *R*-amino acid. Therefore, similarly to the well-studied hydrogenations catalyzed by bis(diarylalkylphosphine) Rh(I) complexes, we conclude that the relative abundance in solution of the diastereomers **13a** and **13b** is not a stereodetermining factor.

(b) Equilibration of Diastereomers of 13. Figure 3 shows the temperature dependence of the ^{31}P NMR spectrum of the

(85) Abu-Hasanayn, F.; Krogh-Jespersen, K.; Goldman, A. S. *J. Am. Chem. Soc.* **1993**, *115*, 8019−8023.

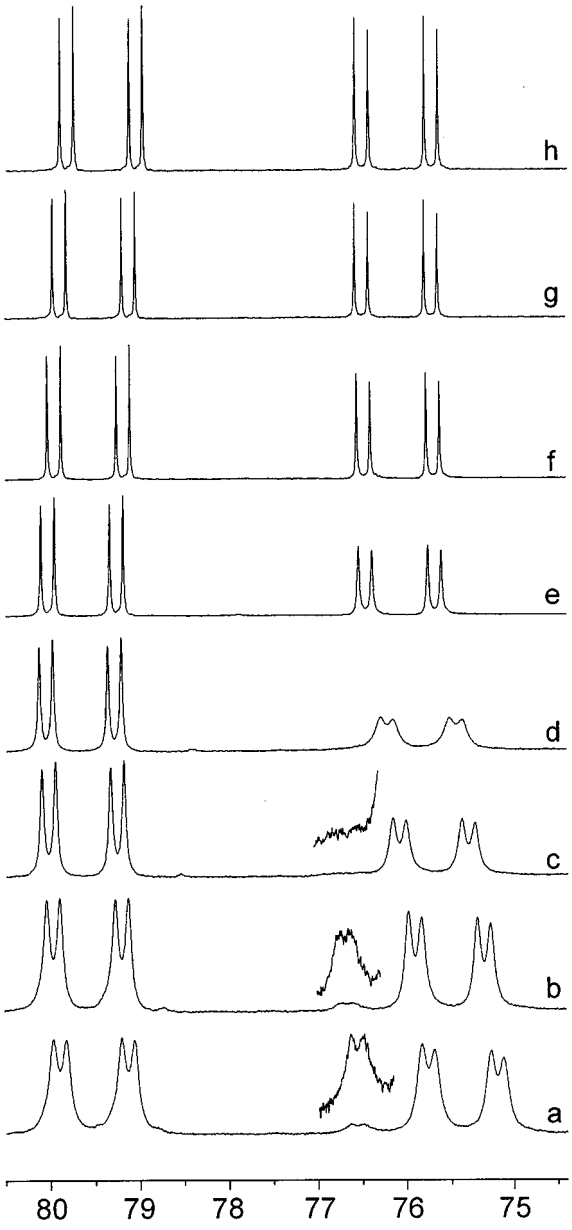

Figure 3. Dependence of the line shape in the ^{31}P NMR spectrum (202 MHz, CD_3OD) of **13** on the temperature: (a) at −95 °C; (b) at −90 °C; (c) at −80 °C, (d) at −72 °C (T_c); (e) at −60 °C, (f) at −50 °C; (g) at 0 °C; (h) at 20 °C.

catalyst−substrate complex **13**. At room-temperature two sharp multiplets of two unequivalent phosphorus atoms were found in the spectrum. Despite the high signal-to-noise ratio, no signals of the second diastereomer could be detected. When the temperature was lowered to −60 °C, a significant broadening of the high-field multiplet was observed. This broadening became maximum at −72 °C, whereas at −95 °C this multiplet sharpened again, and the second signal, apparently of the same multiplicity, appeared (the low-field doublet component of the multiplet is overlapped with the signal of major tautomer). Similar dynamic effects were observed in the ^{1}H and ^{13}C NMR spectra of **13**. These observations indicate the existence of a second species being in fast equilibrium with the major isomer **13a**; equilibrium constant is approximately 10 at −95 °C. This species may be either second diastereomer **13b** or a conformer of **13a**. We cannot distinguish definitely between these two possibilities. The activation barrier is 9 kcal mol^{-1} at $T_C = 201$ K.[86] A very close value of the activation barrier for the intramolecular interconversion of diastereomers of a catalyst−substrate complex was recently reported.[52] By analogy we tend to conclude that the observed temperature dependence of the NMR spectra of **13** corresponds to the fast intramolecular equilibrium between **13a** and **13b** (Scheme 11).

Scheme 11

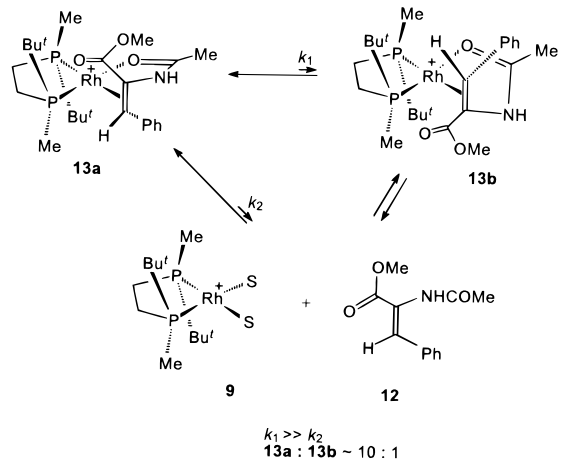

Intensive exchange cross-peaks were observed in the phase-sensitive NOESY spectra of **13** taken in the temperature interval 20−45 °C. The cross-peaks were observed for the exchange between **13** and free substrate **12** and for the pairwise exchange of two methyl and two *t*-Bu groups in the diphosphine-rhodium chelate cycle. Therefore, the EXSY data testify to the reversible dissociation of **13** producing **12** and nondetectable concentration of **9** (Scheme 11). The activation parameters for this reaction ($E_A = 17.4$ kcal mol^{-1}, ln $A = 29$) were found from the quantitative EXSY experiments.[87] Since the intermolecular interconversion of **13a** and **13b** involves this dissociation, we conclude that the barrier for this pathway is much higher than the barrier of the intramolecular interconversion.

(c) Formation of Binuclear Complexes. More complex equilibria were observed if less than 2 equiv of **12** was added to the solution of the solvate complex **9**. The ^{31}P NMR spectra of the samples containing 1, 2, and 0.5 equiv of **12** are compared in Figure 4. When 1 equiv of **12** was added to **9**, then together with the multiplets of **13** and much less intensive broadened doublet of **9**, additional signals were observed in the ^{31}P NMR spectrum (Figure 4b). These are the doublet at 87.0 ppm and two double doublets very close in spectral characteristics to the signals of **13**. The relative intensities of these signals increased notably when only half of an equivalent amount of **12** was added to the solution of **9** (Figure 4a). In the ^{1}H and ^{13}C spectra of the same samples, the signals of an η^6-coordinated phenyl ring were observed (two doublets and three triplets between 5.5 and 7.0 ppm in the ^{1}H spectrum and six signals in the region 90−100 ppm in the ^{13}C spectrum) together with two sets of aliphatic signals similar to those of **13** and **9**. On the basis of the presented evidence, we conclude that a binuclear complex **14** is in equilibrium with **13**, **9**, and **12** (Scheme 12). A second diastereomer, **14b**, with a concentration approximately 10 times lower than that of **14a** was detectable in the ^{1}H and ^{31}P NMR spectra of the equilibrium mixture (e.g.Figure 4a). Apparently, the intramolecular interconversion of **14a** and **14b** is retarded, and both diastereomers can be observed even at ambient temperature.

(86) Sandström, J. *Dynamic NMR−Spectroscopy*; Academic Press: London, 1984

(87) Perrin, C. L.; Dwyer, T. *J. Chem. Rev.* **1990**, *90*, 935−967.

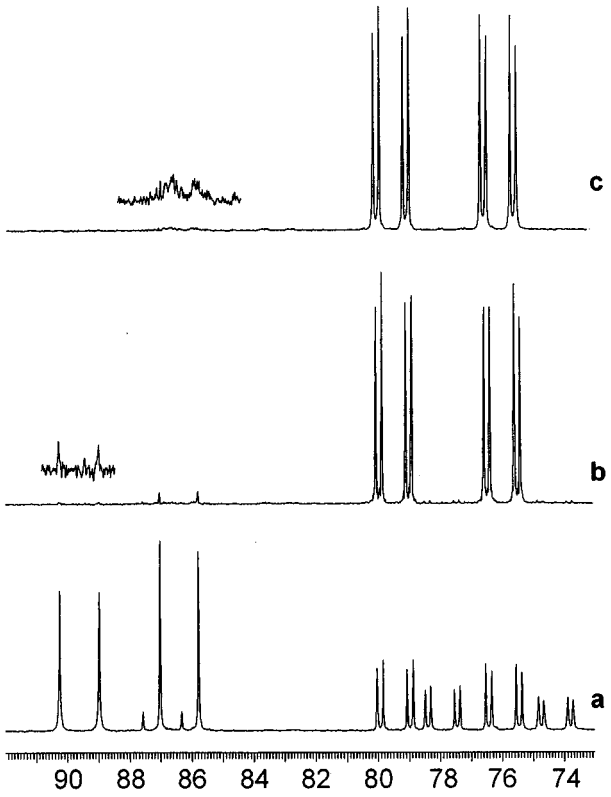

Figure 4. ^{31}P NMR spectra (162 MHz, CD_3OD, −20 °C) of the samples obtained by adding various amounts of **12** to a solution of **9** in deuteriomethanol: (a) 0.5 equiv of **12**; (b) 1 equiv of **12**; (c) 2 equiv of **12**.

Scheme 12

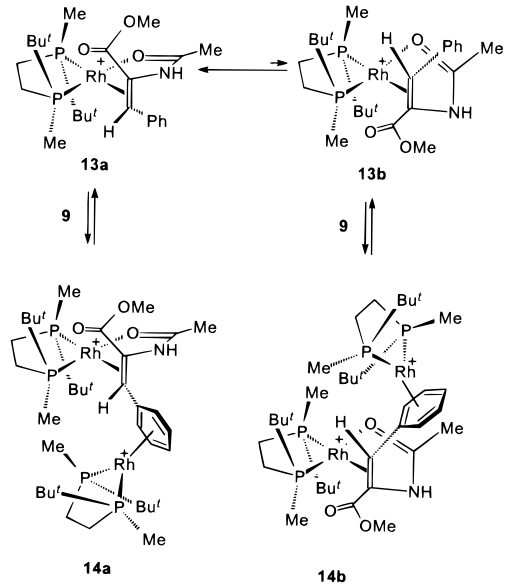

(d) A Catalyst−Product Complex. The solvate complex **9** is capable of coordinating reversibly a molecule of the hydrogenation product **15** (Scheme 13) giving in the ^{31}P NMR spectrum a doublet at $\delta = 87.0$ ($^1J_{Rh-P} = 202$ Hz). The structure of this new species **16** follows from the ^{1}H and ^{13}C NMR spectra containing the signals of the coordinated phenyl ring (5 signals in the ^{1}H NMR in the area 6−7 ppm and 6 signals in the ^{13}C NMR in the region 90−110 ppm), together with the signals of the $CH_2CH(NHCOMe)(CO_2Me)$ moiety very close in spectral characteristics to the hydrogenation product **15** (see Supporting Information for complete NMR data). These spectral data

Scheme 13

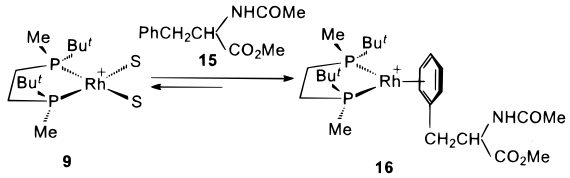

indicate that **16** is a catalyst−product complex in which the product is η^6-coordinated to rhodium by the phenyl ring (Scheme 13).

Such η^6-aryl Rh complexes are not unusual[88−90] and are also known for the chelate diphosphine Rh(I) complexes.[89−92] Surprisingly, this seems to be a first observation of such a complex in the course of the asymmetric hydrogenation. Note that Bargon recently employed PHIP method to detect otherwise nondetectable intermediates similar to **16**.[93]

The equilibrium between **9**, **15**, and **16** was studied in the temperature interval from −80 to +30 °C. The temperature dependence of the equilibrium constant gives for the formation of **16** $\Delta H = -0.7 \pm 0.1$ kcal M^{-1} and $\Delta S = 6.2 \pm 0.3$ cal M^{-1} K^{-1}. Binding of the product **16** is notably weaker than binding of the substrate **12**: in the presence of double excess of **15** a detectable concentration of **9** was observed even at −80 °C.

3. Simulation of the Dihydride Mechanism of Asymmetric Hydrogenation. **(a) Reaction of 12 with Dihydride 10**. Addition of a 2-fold excess of **12** to a solution of dihydride **10** in equilibrium with **9** at −100 °C under hydrogen resulted in immediate disappearance of the signals of **10** from the NMR spectra and appearance of a new hydride species. In the hydride region of the ^{1}H NMR spectrum (Figure 5, compare to Figure 1a) a single multiplet was observed at −23.0 ppm. It correlated to a pair of double doublets at $\delta = 60.2$ and $\delta = 70.4$ in the ^{31}P NMR spectrum. At −50 °C these signals disappeared from the spectra with $t_{1/2} \approx 8$ min and the signals of the hydrogenation product **15**, solvate complex **9**, and η^6-arene complex **16** appeared simultaneously (e.g., Figure 6).

The ^{1}H, ^{13}C, and ^{31}P NMR spectra of this monohydride species **17** (Tables S1−S3) are almost equal to those reported previously for monohydride intermediates.[35,43] The chemical shift of the hydride signal ($\delta_H = -23.0$) indicates its *trans*-disposition to an oxygen atom. The values $^2J_{H,P}$ (16 and 28 Hz) are in agreement with the presence of two *cis*-phosphorus atoms respective to hydride. The signal of the quarternary α-C carbon bound to the rhodium atom has the expected large coupling with *trans*-phosphorus (80 Hz) and a smaller coupling with Rh (20 Hz). The CH_2Ph group resonates at $\delta = 4.09$ in the ^{1}H NMR spectrum and at $\delta = 43.7$ in the ^{13}C NMR. Both carbonyls are approximately 10 ppm downfield-shifted relative to the free ligand (Figure 7) indicating that they both are coordinated to rhodium.[43]

The enantiomeric excess of **15** produced in this experiment was 99% (*R*). Since the migratory insertion step of the

(88) Green, M.; Kuc, T. A. *J. Chem. Soc., Dalton Trans.* **1972**, 832−839.
(89) White, C.; Thompson, S. J.; Maitlis, P. M. *J. Chem. Soc., Dalton Trans.* **1977**, 1654−1661.
(90) Muetterties, E. L.; Bleeke, J. R.; Wucherer, E. *J. Chem. Rev.* **1982**, *82*, 499−525.
(91) Townsend, J. M.; Blount, J. F. *Inorg. Chem.* **1981**, *20*, 269−271.
(92) Singewald, E. T.; Slone, C. S.; Stern, C. L.; Mirkin, C. A.; Yap, G. P. A.; Liable-Sands, L. M.; Rheingold, A. L. *J. Am. Chem. Soc.* **1997**, *119*, 3048−3056.
(93) Hübler, P.; Giernoth, R.; Kümmerele, G.; Bargon, J. *J. Am. Chem. Soc.* **1999**, *121*, 5311−5318.

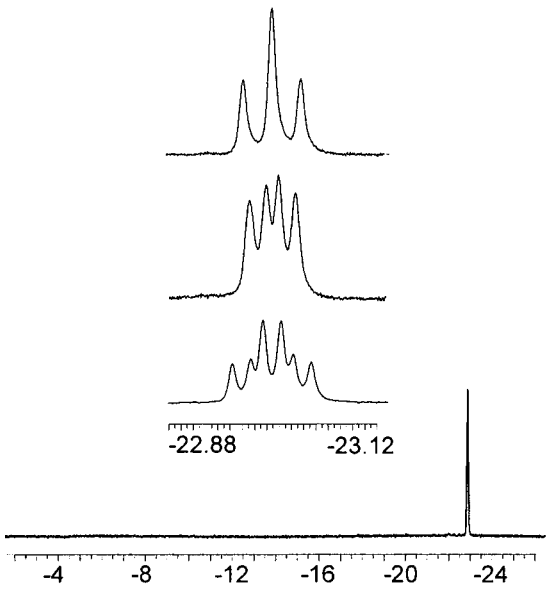

Figure 5. ^{1}H NMR spectrum (600 MHz, CD_3OD, −95 °C) of the sample obtained by addition of a 2-fold excess of **12** to the equilibrium mixture of **9** and **10** at −100 °C. Insets show the appearance of the hydride multiplet with and without selective decoupling from phosphorus.

asymmetric hydrogenation catalyzed by Rh(I) complexes was recently shown to be irreversible,[94] we conclude that the configuration of the α-C in the observed monohydride corresponds to the *R*-hydrogenation product **15**. Furthermore, the structural conclusions based on the NMR data (*cis*-hydride to both phosphorus, α-C *trans* to phosphorus) give reasons to exclude from consideration all possible isomers of **17** except four, viz. **17a**−**d** (Scheme 14). We consider the structures **17c** and **17d** less probable, since neither of them can form directly by the transfer of the equatorial hydride to the coplanar double bond, that is considered to be the nessesary requirement for a successful migratory insertion step.[40,95] The isomers **17a** and **17b** (as well as **17c** and **17d**) can interconvert via dissociation of the Rh−O bond, rotation around the Rh−C bond and recoordination of the carbonyl. The significant low-field shift of both carbonyl carbons in the ^{13}C NMR spectrum of **17** (Figure 7) suggests that they both are coordinated; therefore the isomer **17a** is most probably observed (in **17b** the coordination of the second carbonyl is impossible due to spatial reasons). A ruthenium complex with a very similar coordination of the same substrate was recently characterized by X-ray.[96]

Thus, the reaction of dihydride **10** with **12** proceeds very fast at −100 °C, producing the monohydride intermediate **17a**, which further transforms to the hydrogenation product **15** with 99% ee. This experiment demonstrates the reality of the dihydride mechanism in asymmetric hydrogenation of **12**. Apparently, the dihydride **10** coordinates a molecule of the substrate producing an extremely unstable dihydride intermediate **18** (Scheme 15), which undergoes migratory insertion to produce monohydride **17b**. In **17b** coordination of the second carbonyl is impossible due to geometry reasons and it rearranges to a more stable **17a** by rotation around the Rh−C bond.

(b) Experiments Using HD. Use of HD has been shown to provide valuable information on the mechanism of catalytic

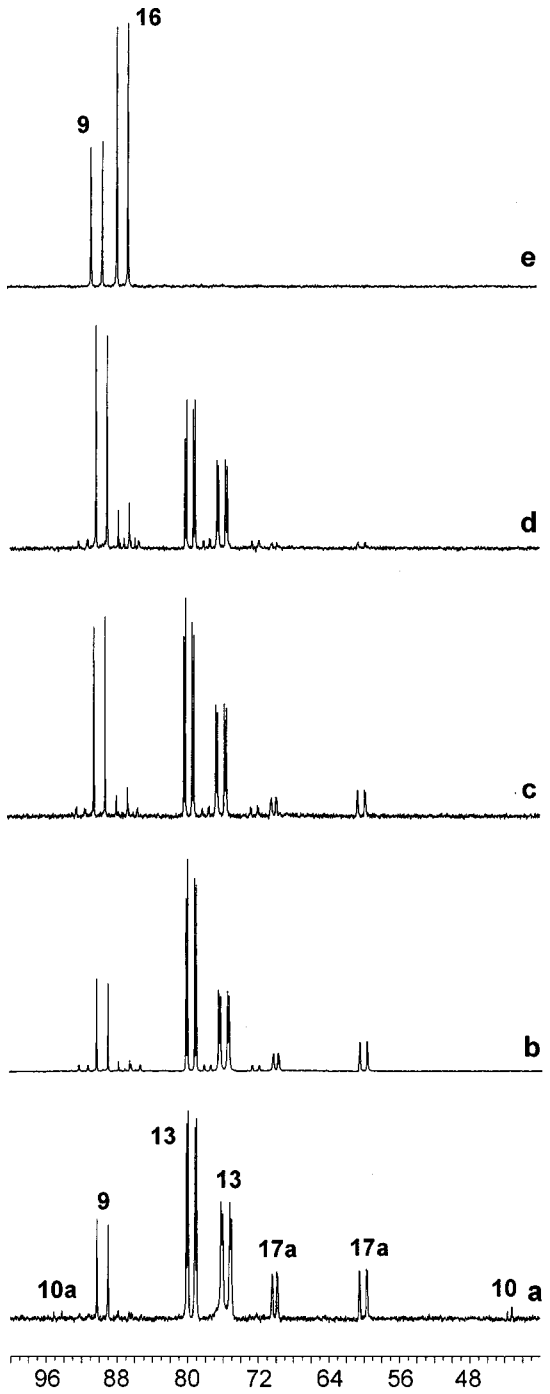

Figure 6. Evolution of the ^{31}P NMR spectrum (202 MHz, CD_3OD) of the sample obtained obtained by hydrogenation of the CD_3OD solution of **13** for 2 h at −80 °C: (a) at −90 °C; (b) at −60 °C; (c) at −50 °C immediately; (d) at −50 °C after 25 min; (e) at 30 °C.

asymmetric hydrogenation.[94,97] The reaction of the mixture of isomers $\mathbf{10^d}$ in CD_3OD gave the isomers $\mathbf{17a^{d1}}$ and $\mathbf{17a^{d2}}$ (the ratio was not determined, since the signal of CH_2 group was obscured by the intensive peaks of **12** and **13**); the ratio of the hydrogenation products obtained after raising the temperature $\mathbf{15^{d1}}$:$\mathbf{15^{d2}}$ was 1.18 (±0.05):1 (Scheme 16).

Catalytic hydrogenation of **12** in CH_3OH using HD with **8** as a catalyst precursor afforded the mixture of two isomers $\mathbf{15^{d1}}$ and $\mathbf{15^{d2}}$ in a 1.17 (±0.05):1 ratio (the mean value from the ^{1}H, ^{2}H, and ^{13}C data). Use of THF as a solvent gave the ratio 1.22 (±0.05):1, which is only slightly higher, and therefore the

(94) Brauch, T. W.; Landis, C. R. *Inorg. Chim. Acta* **1998**, *270*, 285−297.

(95) Seebach, D.; Plattner, D. A.; Beck, A.; Wang, Y. M.; Hunziker, D.; Petter, W. *Helv. Chim. Acta* **1992**, *75*, 2171−2209.

(96) Wiles, J. A.; Bergens, S. H.; Young, V. G. *J. Am. Chem. Soc.* **1997**, *119*, 2940−2941.

(97) Brown, J. M.; Parker, D. *Organometallics* **1982**, *1*, 950−956.

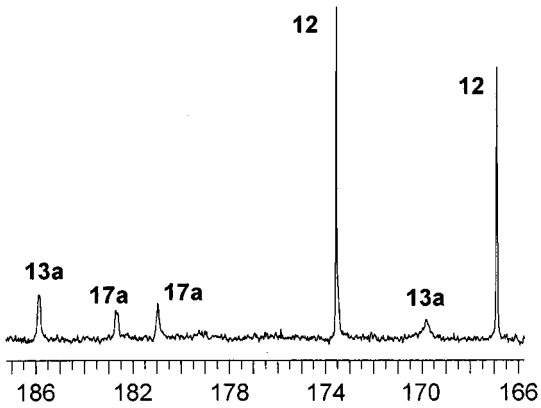

Figure 7. Carbonyl region of a ^{13}C NMR spectrum of a sample containing the mixture of **12**, **13**, and **17a** (100 MHz, CD_3OD, −70 °C).

Scheme 14

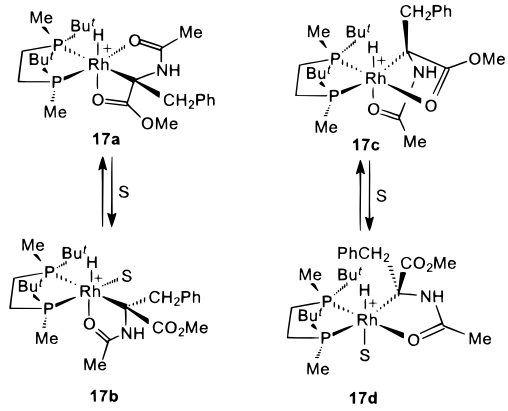

isotopic exchange with the protons of methanol[94] does not affect significantly the observed results. The values of deuterium partitioning for the hydrogenations of **12** catalyzed by DIPHOS,[94,97] DIOP,[97] and DIPAMP[97] are somewhat higher (1.33−1.37); a value close to our results was obtained for the catalytic hydrogenation of methyl acetamidoacrylate.[94]

It is noteworthy that the catalytic hydrogenation and the experiment simulating the dihydride mechanism afforded almost the same value of isotope partitioning. These data suggest that the dihydride pathway is really operating in the catalytic conditions.

Another interesting result is that the preferential occupation of the apical position by deuterium in $\mathbf{10^d}$ is roughly conserved throughout the whole catalytic cycle (Scheme 16). A straightforward explanation of this result is that the partitioning of deuterium on the coordination step and migratory insertion step compensate each other. Calculations predict the partitioning of about 1.5 in favor of α-deuteration for the migratory insertion step.[40] Therefore, to accommodate the observed partitioning to this possibility, the coordination step must give the partitioning order of about 0.6. Besides, the equilibrium between $\mathbf{18^{d1}}$ and $\mathbf{18^{d2}}$ should be faster than the migratory insertion step.

Another possibility to explain the experimental partitioning of deuterium is to suppose that the consequence of substrate coordination and migratory insertion proceeds much faster than the interconversion of $\mathbf{10^{d1}}$ and $\mathbf{10^{d2}}$.

(c) Hydrogenation of the Catalyst−Substrate Complex 13. To simulate more closely the conditions of a catalytic reaction, we have studied the low-temperature hydrogenation of the catalyst-substrate complex **13**. The solution of **13** was hydrogenated under 2 atm of H_2 at −80 °C for 2 h. Analysis of the

Scheme 15

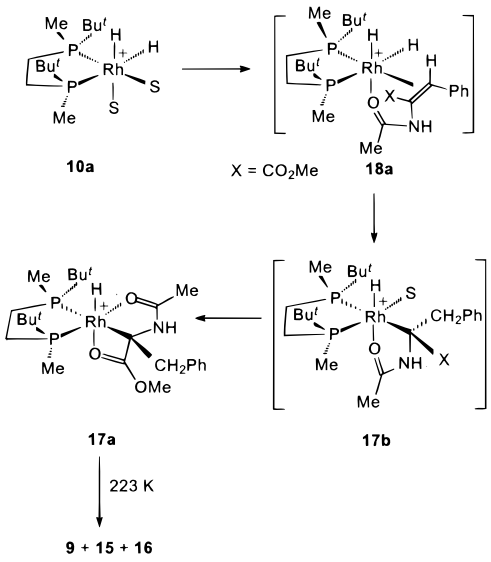

NMR spectra of thus obtained sample (e.g. Figure 6a) showed the high concentration of the monohydride **17a**. Besides, the signals of **9**, **10**, and **13** were found in the NMR spectra. Therefore, the migratory insertion occurs to some extent under the specified conditions, and the liberated catalyst is again hydrogenated producing dihydride **10**, which remains untouched in the absence of additional substrate. When the same experiment was carried out in the presence of 2-fold excess of **12**, a ^{31}P NMR spectrum containing only the signals of **13** and **17a** was obtained. The enantiomeric excess of the hydrogenation product **15** obtained from either of these experiments was 97% (*R*).

It should be mentioned that the formation of the monohydride **17a** upon hydrogenation of **13** was relatively slow: in the reaction between **10** and **12** monhydride **17** was obtained immediately at −100 °C, whereas about 1 h at −80 °C was nessesary to obtain the same concentration of **17a** by hydrogenating **13** under 2 atm of H_2.

Thus, the results of low-temperature hydrogenation of **13** can be also rationalized in terms of dihydride mechanism. In this case the reaction proceeds by reversible dissociation of **13** producing **9** (see above), which is hydrogenated to **10**, which immediately reacts with the substrate. The relatively slow rate of hydrogenation is explained by the slow dissociation step.

On the other hand, nothing speaks against the possibility of a direct hydrogenation of **13**. The rate of equilibration of **13a** and **13b** at −80 °C is high enough to allow the usual explanation of the generation of "correct" monohydride intermediate **17a** from the equilibrium mixture of **13a** and **13b**. Therefore, the simultaneously proceeding unsaturated pathway cannot be ruled out in the asymmetric hydrogenation of **12** catalyzed by **9**. However, the most important fact is the formation of the same monohydride intermediate **17a** and high (*R*)-stereoselection in all three experiments.

4. Mechanism of Asymmetric Hydrogenation Catalyzed by *t*-Bu-BisP* Catalyst and Origin of the Stereoselection. It is possible to rationalize why the different reaction conditions produce the same result in the reaction under study. Indeed, the relative stability of the dihydride **10** implies that a dihydride **18** formed either by reaction between **10** and **12** or by hydrogenation of **13** can easily dissociate to **10** and **12** and produce another diastereomer of **18** in the next association step (Scheme 17). In other words, either complexation of **10** and **12**

Scheme 16

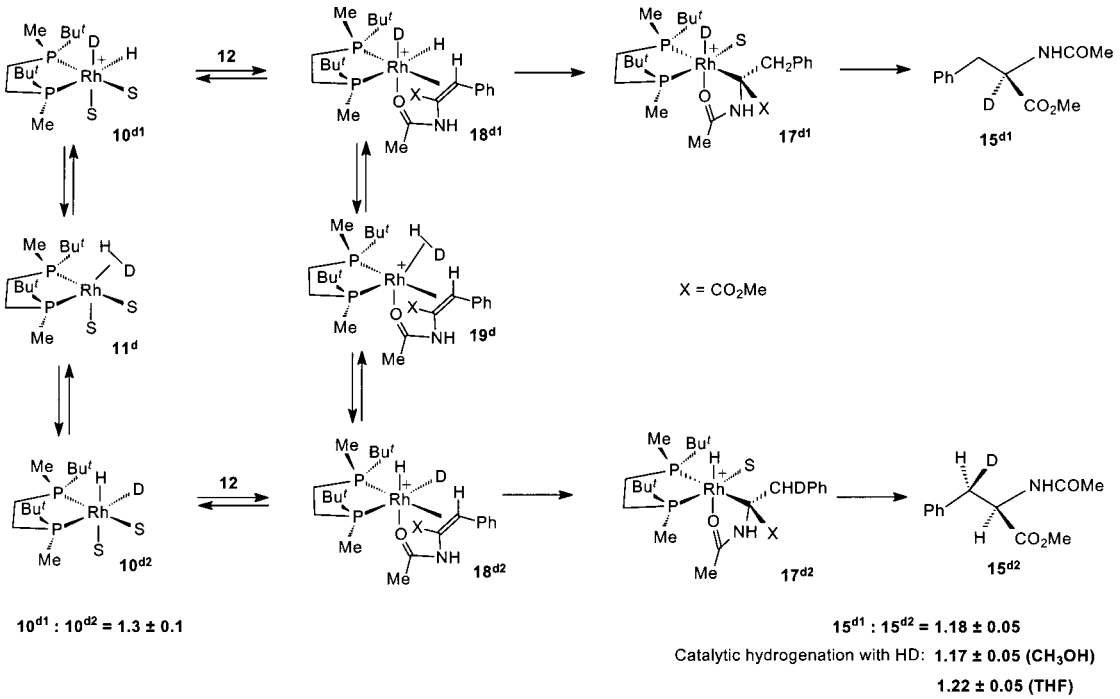

Scheme 17

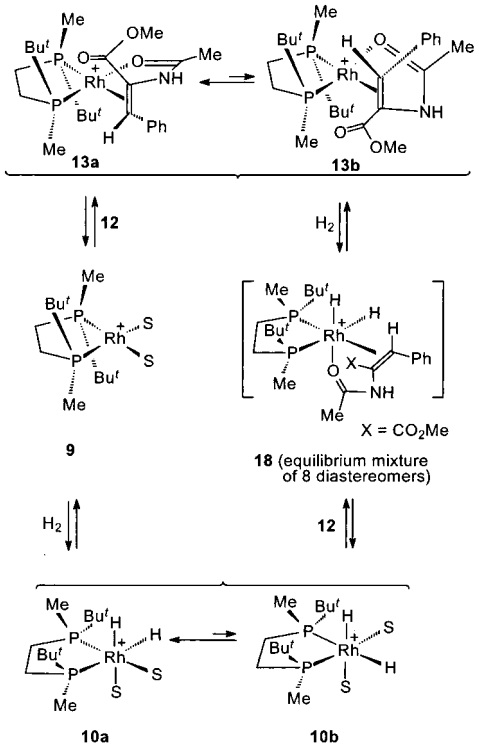

or hydrogenation of **13** produces the same equilibrium mixture of all eight possible diastereomers of **18**. The stereoselection, therefore, must occur at a later step of the catalytic cycle. The same conclusion has been recently made on the basis of computational results for the model systems.[40]

There are eight possible diastereomers of **18**. Only two of these, viz. **18a** and **18b** (Scheme 18) are precursors of the observed α-alkyl monohydride intermediate with *trans*-positioned hydride and oxygen atoms. As can be seen from Scheme 18, the migratory insertion in these intermediates must lead to different stereoisomers of **17**. Our experimantal data together

Scheme 18

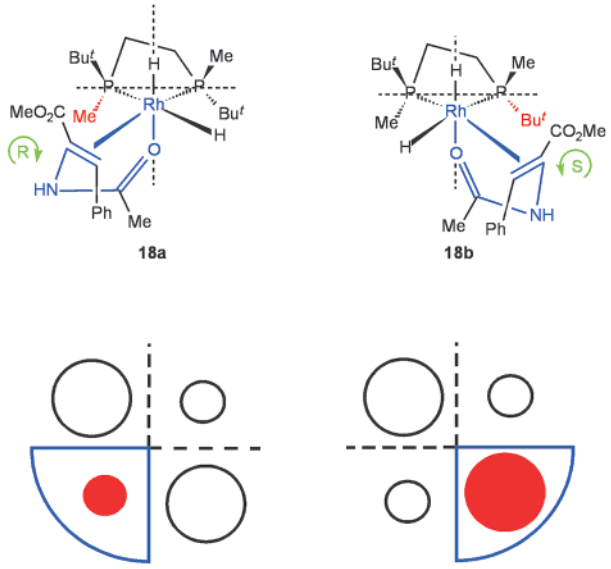

with deuteration experiments[94] and computation results[40] suggest that the migratory insertion is a turnover limiting irreversible step of asymmetric hydrogenation. Therefore, the TS of the migratory insertion should have a geometry similar to that of starting dihydride (Hammond's postulate). Thus, estimating the relative stabilities of **18a** and **18b**, one can roughly compare the barriers of the migratory insertion step.

As can be seen from Scheme 18, the only structural feature discriminating **18a** and **18b** is the nature of the alkyl group being in a close contact with the chelate cycle made by the enamide. In the diastereomer **18a** the chelate ring interacts with the methyl substituent, and in **18b**—with the bulky *tert*-butyl group. It is clear, therefore, that the transition state of the migratory insertion produced from **18a** would be much lower in energy compared to **18b**, and the *R*-stereoselection should be predicted. This corresponds to the experimental findings. Note also that a similar approach was used previously by Seebach et al.[95]

It is interesting to note that coordination of **12** to **10a** produces **18a**, whereas reaction of **10b** and **12** yields **18b**. Therefore, if our assumption of the structure of **10a** is correct, the diastereoselectivity of the hydrogenation of **9** may facilitate the enantioselection in the migratory insertion step.

5. Quadrant Rule. The above considerations on the mechanism of enantioselection are independent of the exact nature of the catalyst. Therefore, following the classification of Knowles et al.,[68,69] we can conclude that any catalyst possesing bulky substituents in the upper-left and lower-right quadrants would produce *R*-hydrogenation products (Scheme 18). The opposite arrangement of substituents would give *S*-products.

This conclusion contradicts the original formulation of the "quadrant rule" made by Knowles for catalysts with backbone chirality and four equivalent or almost equivalent in size phenyl substituents on the phosphorus atoms. It is important to underline that in 1983 Knowles had established the correlation between the spatial arrangement of the substituents and the stereochemical outcome of the reaction. This correlation itself works well: the catalysts with backbone chirality produce *R*-amino acids if in the stable conformation of the rhodium complex upper left and lower right quadrants are occupied with axial phenyls. The opposite arrangement of phenyls gives *S*-amino acids. However, the mechanistic explanation of the quadrant rule proposed in 1983 may be changed in view of the new results obtained recently by us and other workers.

The sense of enantioselection demonstrated by the Rh(I) complexes of P-chirogenic diphosphines, in which the difference in size between four substituents surrounding Rh atom is apparent, is the same as in the case of BisP*. This is valid for the catalysts with BPE,[71] DuPHOS,[71] BIPNOR,[73] CnrPHOS,[74,75] and MiniPHOS[72] ligands. In the case of these ligands the arrangement of substituents in the quadrants is independent of the conformation of the chelate cycle. Therefore, a bulky substituent in the upper left corner (and automatically bottom right for C_2 symmetrical ligand) provokes *R*-stereoselection.

If we apply the latter conclusion for the catalysts with backbone chirality (and accordingly with equal substituents on two phosphorus atoms), we must conclude that *axial phenyls* are recognized as larger ones by the substrate. The relative bulkiness of the *quasi*-axial substituents is understandable in view of Scheme 18, since in the case of octahedral complexes the axial interactions are more important for the stereoselection than the equatorial interactions. The same conclusion has been already made by Nagel in 1989.[59]

We suggest, therefore, that the quadrant rule can be reformulated in a following way: (a) Bulky substituents on phosphorus atoms in the top-left and bottom-right quadrants give *R*-hydrogenation products (Scheme 18); opposite orientation gives *S*-hydrogenation products. (b) If the substituents are the same or very near in size, more steric hindrance is given by *quasi*-axial substituents.

Formulated like this, the quadrant rule remains valid for all catalysts with backbone chirality and is also in accord with the sense of stereoselection demonstrated by new P-chirogenic catalysts for asymmetric hydrogenation.

Conclusions

The profound mechanistic study of the asymmetric hydrogenation catalyzed by BisP*−Rh catalyst revealed several important features of this reaction. The most important finding is the detection and characterization of the dihydride **10**. Because of the lack of experimental evidence on the stability of such dihydrides in the case of diphosphine ligands, the dihydride pathway of the asymmetric hydrogenation was rarely regarded as a serious alternative to the unsaturated mechanism. We have shown, however, that the dihydride mechanism can be successfully simulated at low temperatures by fast and quantitative reaction of the dihydride **10** with substrate **12**, producing the monohydride intermediate **17a**. The same monohydride intermediate **17a** is obtained upon hydrogenation of the catalyst−substrate complex **13**, and the same sense of enantioselection is observed. Our results are completely consistent with the dihydride mechanism of asymmetric hydrogenation catalyzed by $[Rh(BisP^*)S_2]BF_4^-$ (**9**). The enantiodetermining step, therefore, must be the migratory insertion, since on all previous stages of the catalytic cycle the intermediates providing different stereoselection are in equilibrium. We suggest that the main stereodetermining factor is the relative order of steric repulsion between the chelate ring made by the substrate and the alkyl substituent on phosphorus in two isomers of a dihydride intermediate (**18a** and **18b**). The proposed mechanism of stereoselection is consistent with the sense of enantioselectivity demonstrated by the catalysts with P-chirogenic ligands. The generally applicable quadrant rule may be formulated by accepting the larger steric hindrance of the *quasi*-axial phenyls for the catalysts with backbone chirality

Acknowledgment. This work was supported by "Research for the Future" Program, the Japan Society for the Promotion of Science, the Ministry of Education, Japan.

Supporting Information Available: Experimental procedures for **8**−**10**, **13**, **14**, **16**, and **17**; Tables S1−S3 of NMR data for **9**, **10**, **13**, **14**, **16**, and **17**; charts of ^1H, ^{13}C, and ^{31}P NMR spectra and 2D NMR of **8**−**10**, **13**, **15**−**17**, **10^d**, and **15^d**; linearized dependencies of equilibrium constants versus temperature for **10**, **10^d**, and **16**; kinetic data for **13**. This material is available free of charge via the Internet at http://pubs.acs.org

JA000813N